Available online at www.sciencedirect.com

SciVerse ScienceDirect

Physics Procedia 39 (2012) 327 – 335

Physics Procedia

LANE 2012

Parameter influence on Surfi-Sculpt processing efficiency

Caroline Earl[a,b,*], Paul Hilton[b], Bill O'Neill[a]

[a]*Centre for Industrial Photonics, Institute for Manufacturing, The University of Cambridge, Cambridge, CB3 0FS, United Kingdom*
[b]*TWI Ltd., Granta Park, Abington, Cambridge, CB21 6AL, United Kingdom*

Abstract

The three-dimensional laser surface modification manufacturing technique, Surfi-Sculpt®, is thought to be driven by a melt pool instability that is dependent on a quasi steady-state temperature field. The melt pool instability can be controlled through a greater understanding of the heat input and selection of optimised laser processing parameters. This in turn enables the optimum production of a range of feature shapes, so that this new manufacturing technique can be applied in applications requiring increased surface area of the substrate or functional surface textures.

© 2012 Published by Elsevier B.V. Selection and/or review under responsibility of Bayerisches Laserzentrum GmbH
Open access under CC BY-NC-ND license.
Keywords: Process Optimisation; High Speed Imaging; Thermal Imaging; Instabilities; Humping; Surface Structure

1. Motivation

Laser surface modification offers applications to areas including: bonding [1], heat exchange [2], biomedicine [3], surface wetting [4] and tribological improvements [5]. Surface features produced by the Surfi-Sculpt process are difficult, or impossible to manufacture by any other method. Surfi-Sculpt also has the advantage of increasing the surface area without the addition of material. Surfi-Sculpt can be utilised to enhance the functional properties of materials; increasing the surface area for thermal energy exchange in addition to controlling the dynamics of fluid flow over a surface from laminar to turbulent. Heat exchanging applications have demonstrated a combination of benefits including a 50% increase in the measured heat transfer coefficients across a range of fluid flow rates [6].

* Corresponding author. Tel.: +44-122-376-6141 ; fax: +44-122-346-4217 .
E-mail address: cle36@cam.ac.uk .

1875-3892 © 2012 Published by Elsevier B.V. Selection and/or review under responsibility of Bayerisches Laserzentrum GmbH
Open access under CC BY-NC-ND license. doi:10.1016/j.phpro.2012.10.045

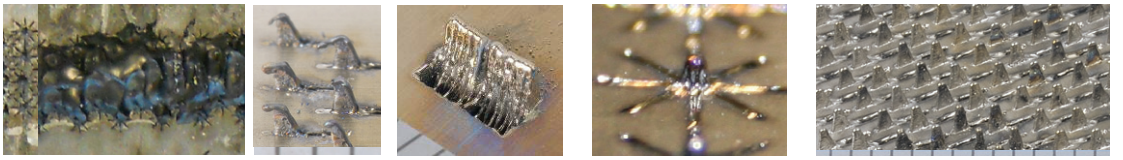

Fig. 1. (a) Rubber bonding onto metal stars; (b) Hooks; (c) Wall; (d) 8-leg star feature; (e) Array of single features.

Wider manufacturing applications are offered by the possibility of bonding different material groups such as composite to metal bonding or for promoting coating adhesion. By optimising parameters of the Surfi-Sculpt process, features have been produced for rubber to metal bonding (see fig. 1a). Other possible applications that are well suited to the technique are 'hook and loop' joining mechanisms, fig. 1b. Surfi-Sculpt can be tailored to produce a textured surface along the sides of the features, so that the surface forms additional hooks which can join to a fibrous material. Developments in scanning and laser technology reduce costs and increase production rates so that the possibility of applying the laser Surfi-Sculpt techniques becomes increasingly feasible.

Surface features are produced by molten displacement generated by repeated swipes of a focused laser beam. The features are characterised by a protrusion and corresponding intrusion, fig. 2. There is a critical time delay and feature spacing between each of the swipes in order to achieve the quasi steady-state temperature conditions and optimized melt displacement. This work investigates the relationship between the thermal conditions and feature production.

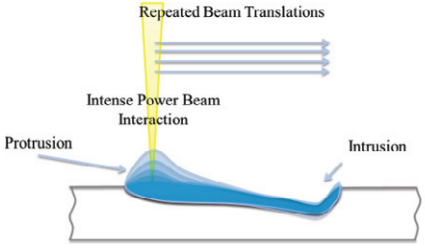

Fig. 2. Surfi-Sculpt process mechanism

It is thought that surface features are formed by a combination of the resulting vapour pressure from the keyhole and a thermally driven surface tension gradient along the swipe length [7]. The process is thought to be similar to that of the humping phenomenon observed in high speed laser welding [8]. In particular, the 'keyhole' and 'fluid dynamically' dominated regimes, are dependent on the interaction between the vapour jet from the keyhole formation and the melt, which are a strong function of the melt flow velocity. At higher velocities the melt no longer impacts the vapour jet [9]. The two mechanisms were previously observed in the Surfi-sculpt process by the stabilisation of surface oscillations at higher welding speeds [8].

2. Experimental

A single mode fibre laser operating at 1.07μm was used for all experiments. This was scanned across the material using a glavometer based ARGES Elephant scanner and lens focusing system. The beam caustic derived minimum spot size and divergence angle were measured at 86% of the intensity point at 23 μm and 39 mrad respectably, with a beam parameter product (BPP) of 0.5 mm*mrad. The measured Rayleigh length at 86% radius was 1.18 mm. The substrate material was Ti-6Al-4V. Processing was

carried out in an argon atmosphere, within a base fed enclosed chamber. This gave a low oxygen content of 0.07% in the process region, under an optimised argon flow rate of 1 l/min to minimise oxidation. The beam focus position was varied using the three-dimensional z-axis capability of the ARGES scanner.

High-speed imaging was carried out to examine build rates using a shadowography technique, fig. 3a and b, with a Vision Research V710 camera at 15,000 fps, and a Motion Pro YS1 PIV and Vision Research V7.3, at 1,000 fps. The process was illuminated by a 500W Cavilux HF laser operating at 810 nm wavelength. A 1µm band-pass filter was set in front of the high-speed camera in order to eliminate stray laser light and enhance the image quality.

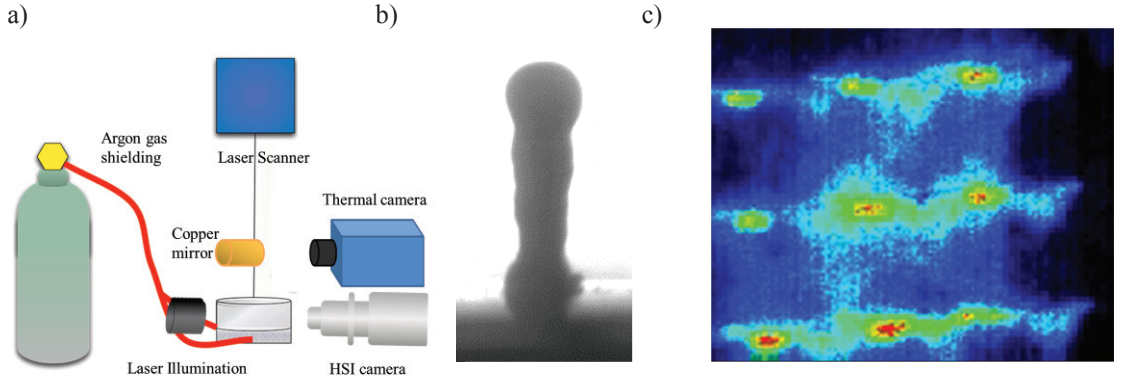

Fig. 3. (a) Experimental set-up; (b) HSI shadowography profile; (c) Thermal image of array production

Simultaneously a high frame-rate infrared (CEDIP Titanium) camera was used at 2000Hz to capture raw IR data for each laser swipe in order to study the temperature distribution of the melt pool and thermal build up rates, fig. 3. A concave copper mirror (f=330mm) was used to enable the image to be reflected away from the point of processing, reducing the risk of damage to the camera, this only gave a 0.355% loss of thermal data with the emissivity calibrated to 0.56 [10]. Argon shielding was provided by an open base fed container at 25 l/min.

Design of experiment analysis (DOE) [11] was used to identify the most important processing parameters when producing 8 legged star features, fig. 1d. Data was entered historically and modelled using response surface methodology, to investigate optimums and relevant interactions between variables. A cubic model with a square root transformation gave the best fit to the data. The time delay and swipe length were kept constant with the interacting parameters shown in table 1 chosen for investigation. Initial screening trials were carried out to identify the relevant focal ranges for each of the power values investigated. The focal distance is defined as 'the distance between the laser focal point and the processing surface' as shown in fig. 4.

Table 1. Processing parameters

Parameter	Range	
Laser Power beam (W)	200	1000
Laser translation speed (mm s^{-1})	200	1800
Focal distance (mm)	-42	+6

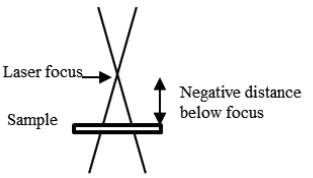

Fig. 4. Measurement of a negative focal distance

3. Results and Discussion

3.1. *Parameter to feature height relation*

Analysis of variance from the DOE showed the focal distance to be the most significant factor for maximising height, followed by the laser translation speed, then laser power. Interactions were observed between focal distance and speed and also power and square of the speed. This reinforces the significant importance of the melt volume generated by the power density and spot size, relative to the melt flow.

Results shown in fig. 5 identify, irrespective of the focal position, that there is a complex relationship between processing speed and laser power. At large negative focal distances the process seems completely dependent on the power density required, as there is a lack of feature production at low powers and high speeds. At high powers, low speeds and smaller focal distances, overheating occurs and the quasi steady-state temperature field is no longer achieved.

At lower power levels, irrespective of the speed, there is a peak in the process. The power value at which this occurs, shifts towards lower powers as the focal position tends towards zero and the spot size is decreased, indicating a power density relation in this shift. It appears that the production mechanism is "keyhole dominated" and is caused by the direct impact of the vapour jet on the melt.

At higher power levels, speed has a much greater influence, since at low speeds the process becomes unstable with vaporisation and spatter occurring. At higher speeds it is thought that the process becomes "fluid dynamically" driven rather than experiencing a keyhole melt pool interaction instability. The faster melt flow in the side wall streams merges at a distance further from the keyhole front. The melt pool length would also increase with increased power input and speed. As described in [12], when the melt pool lengthens the hump is able to absorb more surface waves, enabling greater feature volume.

The region between the two domains of operation may indicate a lack of melt for the fluid dynamic regime to be significant, or a conflicting process of the two mechanisms operating simultaneously, as previously observed [9]. A deconstructive interference of the melt flow vectors from the keyhole and side wall stream could also cause the lack of humping within this operating region.

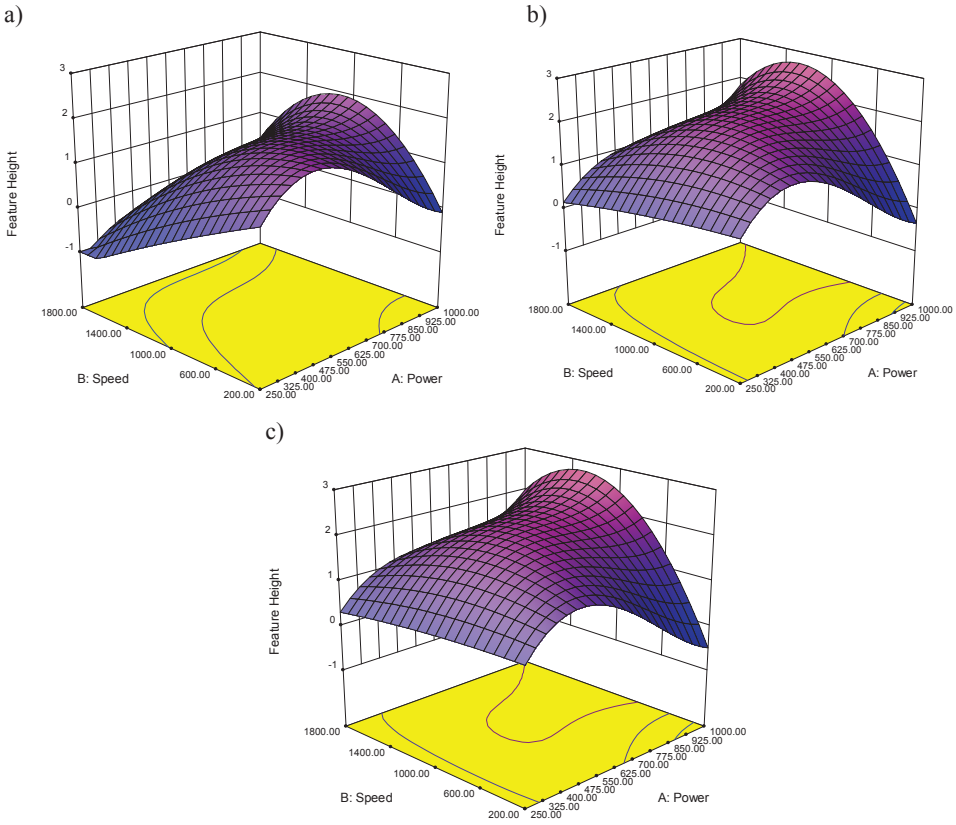

Fig. 5. Relation between speed and power on Ti-6Al-4V at focal distances of (a) -20 mm (b) -10 mm and (c) 0 mm

3.2. *Feature build rates*

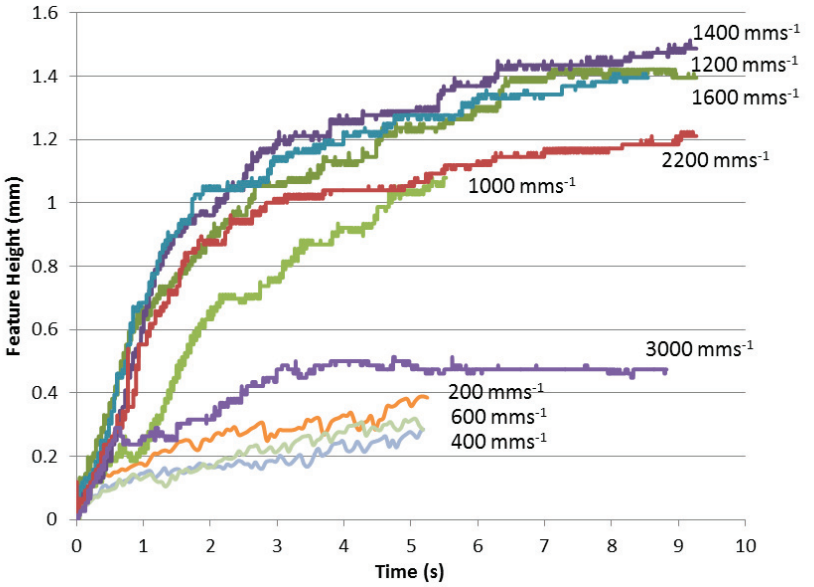

Fig. 6. Influence of processing speed on the build rate of feature

The two regimes of operation have also been identified when analysing the build rates of feature height increase with time at different speeds, as shown in fig. 6, from shadowography data as shown in fig. 3b. The result at 200 mm s^{-1} shows a good production rate relative to slightly higher speeds such as 400 and 600 mm s^{-1}. The graph also shows that above a speed of 1100 mm s^{-1} the initial build rate is very consistent and appears to "lock in" to a steady production mode. This remains until the speed is increased to over 2200 mm s^{-1} when it is presumed that the power density is no longer high enough to support the fluid dynamically driven mode.

3.3. *Quasi–steady thermal state*

When considering the production of arrays of features the quasi-steady thermal state becomes even more important. Factors that greatly influence the surrounding thermal environment are the delay time, array size and array distribution.

Fig. 7 shows the effect of array size on the heat build-up over areas identical in size when producing single legged features, as shown in fig. 1e, 3mm apart in arrays of 2 x 2 and 3 x 3. Despite more features being built in the 3 x 3 array, the thermal build up rate is shown to be much greater for the 2 x 2 array where there is less time for the heat to be conducted away from an area before the laser returns to that area.

When using the same delay time as occurred naturally from array production to producing single features the thermal build up seemed un-affected by the different delay times, fig. 8.

It is therefore thought to be the intensity of returns to an area and therefore surrounding thermal influences that have a greater impact on the thermal build-up rate, rather than the time between each return of the laser. Features are also larger in the cooler thermal state from the larger array and indicate overheating with the appearance of a bobble on top of the feature produced in the 2 x 2 array.

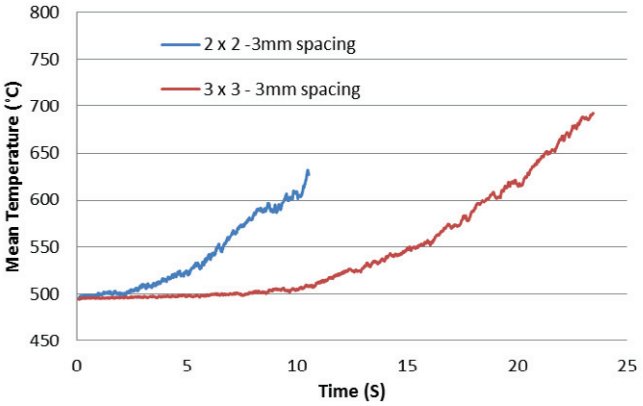

Fig. 7. Thermal build-up in array production of different sizes

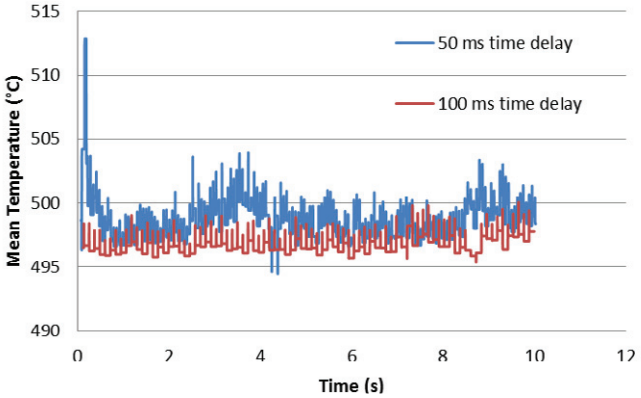

Fig. 8. Thermal build-up in single feature production with different delay times

3.4. *Increased production rates*

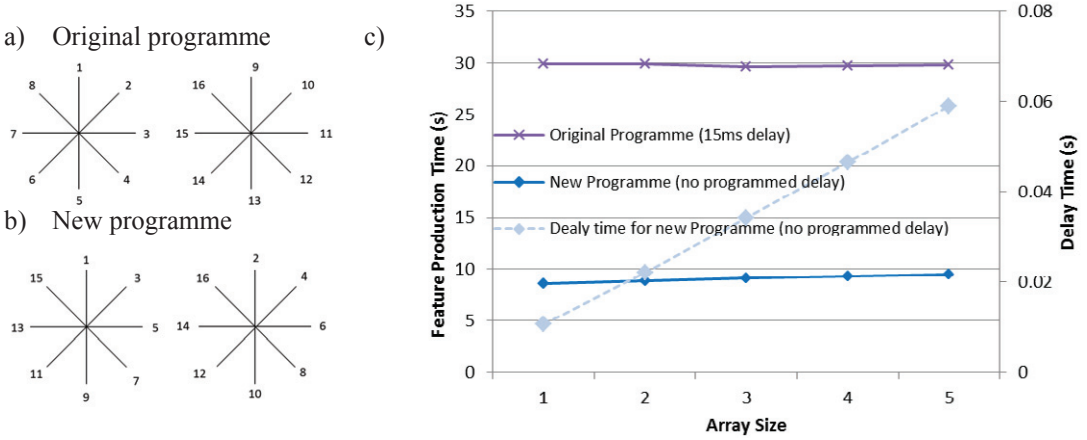

Fig. 9. For 8 legged pattern: (a) Original programming sequence; (b) New programming sequence; (c) 25% reduction in production time with new programme for features with 8 legs and 100 swipe repeats. Array size represents the base size, e.g. 2 = 2 x 2 array

By understanding the effect of thermal conditions on the process it has been possible to programme the software to operate as efficiently as possible. The new programme achieves this by providing the cooling time required by processing on other areas of the material, instead of having a delay.

For an 8-legged feature, the new production shows a 75% reduction compared to the original production time, fig. 9. Single legged features achieve even better results: a 3 x 3 array of single features built with 250 swipes initially took 288 seconds and now takes 24.332 seconds. This is 8.45% of the original time. As shown in fig. 6 the majority of the build, about 70%, occurs with the first 2 seconds. When a smaller height is required, the build time can be as little as 1.083 seconds per single feature of 0.93mm. The relation between production time for a single feature and height is shown in fig. 10. Trials on thicker materials have shown that, at longer processing times, the height is restricted by overheating rather than by a shortage of material.

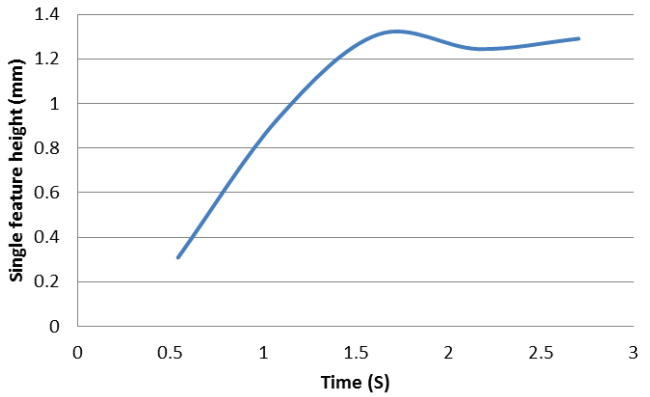

Fig. 10. Feature heights of a single feature achieved with increasing processing times

3.5. *Material conservation*

One of the main advantages of the process is that no additional material is required to produce the features. Surface profilometry of the protrusion and corresponding intrusion have been compared, fig. 11, and give an average ratio of 1.025, with a slightly greater area in the protrusion. This is possibly due to thermally induced residual stresses and/or a very small oxide content. Further experimentation will be carried out to investigate this.

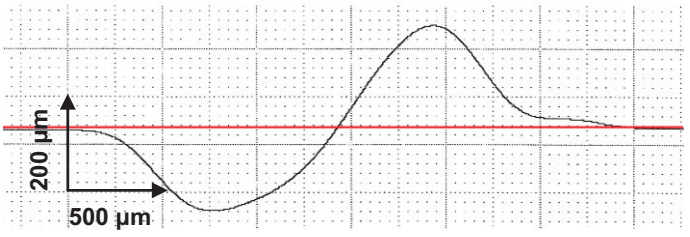

Fig. 11. Surface profile of a protrusion and intrusion of a feature formed with 50 swipes

4. Conclusions

- Keyhole dominated and fluid dynamically driven regimes of operation have been identified.
- Processing speed is shown to have a significant influence on feature build rate.
- Quasi-steady thermal state has been shown to be influenced more by the surrounding array than the delay time.
- Improvements in thermal management have reduced array production times and single features can now be produced in 1.083 seconds for a feature 0.93mm in height.
- Material conservation is measured at a ratio of 1.025 with a slight increase in the protrusion area.

Acknowledgements

This work is funded by the EPSRC and TWI Ltd. The authors would like to thank the EPSRC Engineering Instrument Loan Pool and Peter Anthony for the loan of the high speed thermal imaging camera. Also, thanks to Kai Hsiao (Inkjet research centre, IfM) and David Rudeforth (IDT Ltd.) for the loan of the HSI cameras.

References

[1] Baburaj, E.; Starikov, D.; Evans, J.; Shafeev, G.; Bensaoula, A.: Enhancement of adhesive joint strength by laser surface modification. In: International journal of adhesion and adhesives, 27 (2007), 268-276.

[2] Adjim, M.; Pillai, R.; Bensaoula, A.; Starikov, D.; Boney, C.; Saidane, A.: Thermal analysis of micro-column arrays for tailored temperature control in space. In: Journal of heat transfer, 129 (2007), 798-804.

[3] Kurella, A.; Dahotre, N. B.: Review paper: surface modification for bioimplants: the role of laser surface engineering. In: Journal of biomaterials applications, 20 (2005), 5-50.

[4] Bizi-Bandoki, P.; Benayoun, S.; Valette, S.; Beaugiraud, B.; Audouard, E.: Modifications of roughness and wettability properties of metals induced by femtosecond laser treatment. In: Applied Surface Science, 257 (2011), 5213-5218.

[5] Hu, Y. Z.; Ma, T. B.: 3.12 - Tribology of Nanostructured Surfaces. In: Comprehensive Nanoscience and Technology, L. A. Editors-in-Chief: David;D. S. Gregory;P. W. Gary, Editors. Academic Press: Amsterdam.383-418 pp.

[6] Buxton, A. L.; Ferhati, A.; Glen, R. J. M.; Dance, B. G. I.; Mullen, D.; Karayiannis, T.: EB Surface Engineering for High Performance Heat Exchangers. Proc. First International Electona Beam Welding Conference, Chicago, IL, USA (2009).

[7] Hilton, P.; Jones, I.: A new method of laser beam induced surface modification. In: The Laser User, (2008), 46-49.

[8] Earl, C. L.; Hilton, P.; O'Neill, W.: A Comparative study of 3D laser surface modification and the humping phenomenon. Proc. ICALEO, Orlando, Florida, USA (2011).

[9] Berger, P.; Hügel, H.; Hess, A.; Weber, R.; Graf, T.: Understanding of Humping Based on Conservation of Volume Flow. In: Physics Procedia, 12 (2011), 232-240.

[10] Boivineau, M.; Cagran, C.; Doytier, D.; Eyraud, V.; Nadal, M. H.; Wilthan, B.; Pottlacher, G.: Thermophysical properties of solid and liquid Ti-6Al-4V (TA6V) alloy. In: International journal of thermophysics, 27 (2006), 507-529.

[11] Montgomery, D. C.: Design and Analysis of Experiments. John Wiley & Sons, Inc., Hoboken, 2005.

[12] Tsukamoto, S.; Irie, H.; Inagaki, M.; Hashimoto, T.: Effect of Focal Position on Humping Bead Formation in Electron Beam Welding. In: Trans. Natl. Res. Inst. Met.(Jpn.), 25 (1983), 62-67.